

Density effect on hadronization of a quark plasma

P. Zhuang, M. Huang, and Z. Yang

Physics Department, Tsinghua University, Beijing 100084, China

(Received 11 January 2000; published 25 September 2000)

The hadronization cross section in a quark plasma at finite temperature and density is calculated in the framework of the Nambu–Jona-Lasinio model with explicit chiral symmetry breaking. In contrast to the familiar temperature effect, the quark plasma at high density begins to hadronize suddenly. It leads to a sudden and strong increase of final state pions in relativistic heavy ion collisions which may be considered as a clear signature of chiral symmetry restoration.

PACS number(s): 12.38.Mh, 25.75.-q, 11.10.Wx, 24.85.+p

I. INTRODUCTION

It is generally believed that there are two QCD phase transitions in hot and dense nuclear matter [1]. One of them is related to the deconfinement process in moving from a hadron gas to a quark-gluon plasma, and the other one describes the transition from the chiral symmetry breaking phase to a phase in which it is restored. Theoretical evidence from lattice simulations [2] of QCD at finite temperature for these phase transitions has prompted experimental efforts to create the new phases of matter in the laboratory during the early stages of relativistic heavy ion collisions. Since it is still difficult to extract definite information about the phase transitions from the lattice simulations with nonzero baryon density, we need QCD models to investigate the phase transitions at finite density. From a recent study [3] based on the instanton model, the phase structure is more rich at high density than at high temperature. There exists a new phase of color superconductivity when the density is sufficiently high.

Chiral symmetry plays a crucial role for the behavior of light hadrons in determining not only their static properties in the vacuum, but also the changes therein that are due to in-medium effects. One of the models that enables us to see directly how the dynamic mechanisms of chiral symmetry breaking and restoration operate is the Nambu–Jona-Lasinio (NJL) model applied to quarks [4]. Within this model, one can obtain the hadronic mass spectrum and the static properties of mesons remarkably well. In particular, one can recover the Goldstone mode and some important low-energy properties of current algebra such as the Goldstone-Treiman and Gellmann-Oakes-Renner relations. Because of the contact interaction between quarks that is introduced in the model, there is of course no confinement. A further consequence of this feature is that the model is nonrenormalizable, and it is necessary to introduce a regulator Λ that serves as a length scale in the problem, and which can be thought of as indicating the onset of asymptotic freedom.

At low baryon density, the phase transition of chiral symmetry restoration in the chiral limit is of second order in the case with quarks of nonzero mass it becomes a smooth crossover as a function of temperature and density. This picture obtained in the NJL model with two flavors is consistent with present lattice simulations and many models [5]. However, at high density several models [3,4] suggest that the chiral symmetry restoration transition is of first order. Assuming that this is the case in QCD, this first-order transition

will remain in the case in which explicit chiral symmetry breaking is present. This raises the possibility that some consequences of chiral symmetry restoration obtained in the chiral limit may be found in the real world with massive pions. Some authors [6] have discussed the signatures of a first-order phase transition, such as the event-by-event rapidity fluctuations and the associated variations in Hanbury Brown–Twiss (HBT) radii.

In relativistic heavy ion collisions, nuclear matter is first heated and/or compressed up to a region of both a chirally symmetric and a deconfined phase of matter, and then in the cooling process the deconfined partons will recombine into the observed hadrons, which are mainly pions. It is important to understand how a quark plasma converts into a hadron gas at finite temperature and density, and especially what the influence of the chiral symmetry restoration transition is on the hadronization process. Although we are aware of the disadvantages of the NJL model, the lack of confinement and nonrenormalizability of the effective four-fermion interaction, its strengths, the transparent description of the chiral phase transition, and the binding of quarks into mesons, it is worthwhile to discuss the effect of chiral phase transition on the hadronization rate in this model. From a study [7] of the hadronization rate for the conversion of a quark-antiquark pair into two pions, $q\bar{q} \rightarrow 2\pi$ at zero baryon density and, in the chiral limit, the hadronization cross section diverges at the critical temperature T_c of the chiral phase transition. Since the phase transition at low density will be fully washed out when explicit chiral symmetry breaking is taken into account, the dynamic divergence will no longer exist in the real world. A natural question is whether any information about the chiral phase transition at high density is retained in the hadronization rate when a nonzero current quark mass is considered. In this paper, we investigate at finite temperature and density the hadronization rate for $q\bar{q} \rightarrow 2\pi$ in the flavor SU(2) NJL model with explicit chiral symmetry breaking.

The paper is organized as follows. In Sec. II, we briefly review the quarks at the mean field level and mesons within the random phase approximation (RPA). We discuss especially the phase diagrams of the model in temperature-chemical potential (T - μ) plane and temperature-baryon density (T - n_b) plane. In Sec. III, we study the behavior of the hadronization cross section to first order in a $1/N_c$ expansion as a function of the c.m. energy s , temperature T , and baryon density n_b . We focus our attention on the difference between temperature and density effects, and the influence of the chi-

ral phase transition on the hadronization rate. We summarize in Sec. IV.

II. PHASE DIAGRAMS

The two-flavor version of the NJL model is defined through the Lagrangian density

$$L_{NJL} = \bar{\psi}(i\gamma^\mu\partial_\mu - m_0)\psi + G[(\bar{\psi}\psi)^2 + (\bar{\psi}i\gamma_5\tau\psi)^2], \quad (1)$$

where only the scalar and pseudoscalar interactions corresponding to σ and π mesons, respectively, are considered, ψ and $\bar{\psi}$ are the quark fields, τ is the SU(2) isospin generator, G is the coupling constant with dimension GeV^{-2} , and m_0 is the current quark mass.

The key quantity for dealing with the thermodynamics of a variable number of particles is the thermodynamic potential Ω . In the mean field approximation, which is the lowest order $O(1)$ in the $1/N_c$ expansion, it is [8]

$$\begin{aligned} \Omega(T, \mu, m_q) &= \frac{(m_q - m_0)^2}{4G} - 2N_c N_f \int \frac{d^3\mathbf{p}}{(2\pi)^3} E_p - 2N_c N_f T \\ &\times \int \frac{d^3\mathbf{p}}{(2\pi)^3} \ln(1 + e^{-(E_p + \mu)/T}) \\ &\times (1 + e^{-(E_p - \mu)/T}), \end{aligned} \quad (2)$$

where $E_p^2 = \mathbf{p}^2 + m_q^2$, μ is the chemical potential, and N_c and N_f are the number of colors and flavors, respectively. Equation (2) holds for any value of the quark mass m_q , which is the order parameter of the chiral phase transition. In the spirit of thermodynamics, the physical system is described by that value of m_q for which $\Omega(T, \mu, m_q)$ is a minimum,

$$\frac{\partial\Omega}{\partial m_q} = 0, \quad \frac{\partial^2\Omega}{\partial m_q^2} \geq 0. \quad (3)$$

The above equality is the so-called gap equation to determine the constituent quark mass as a function of T and μ . The inequality is especially necessary in the high-density region where the thermodynamic potential has two minima and one maximum.

In the chiral limit when the current quark mass $m_0 = 0$, the solution of the gap equation separates the region of chiral symmetry breaking with $m_q \neq 0$ from the region of chiral symmetry restoration with $m_q = 0$. The phase-transition lines demarcating these two regions are given in Fig. 1(a) in the T - μ plane and Fig. 1(b) in the T - n_b plane. The relation between the baryon density n_b and the chemical potential μ is rather complicated and is also a function of T ,

$$n_b = \frac{N_c N_f}{3} \int \frac{d^3\mathbf{p}}{(2\pi)^3} \left[\tanh \frac{1}{2T} (E_p + \mu) - \tanh \frac{1}{2T} (E_p - \mu) \right], \quad (4)$$

where the factor of 3 reflects the fact that three quarks make a baryon.

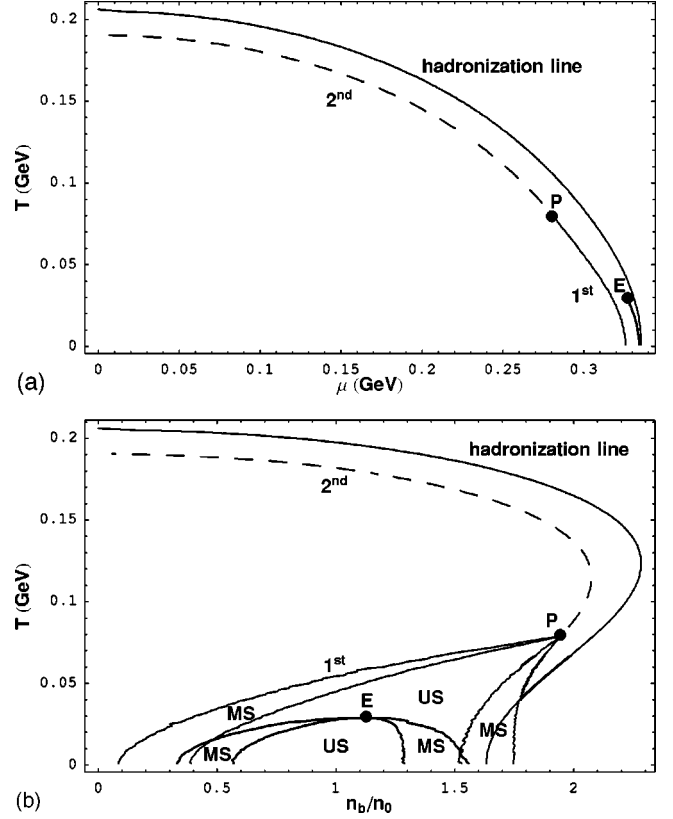


FIG. 1. The phase-transition line and hadronization line in the T - μ plane (a) and T - n_b plane (b). The dashed lines indicate a second-order transition while the thin solid lines indicate one of first order in the chiral limit. The point P is tricritical. The thick solid lines with critical end point E are the lines of first-order transition with nonvanishing current quark mass. For the first-order transition with and without current quark mass, the mixed region is divided into unstable (US) and metastable (MS) regions. The hadronization line separating the region of quark plasma from that of quark-meson plasma is indicated by thin solid lines in the two planes.

The order of the chiral phase transition is determined by the behavior of the order parameter across the phase-transition line. If the quark mass m_q is continuous, the phase transition is of second order, indicated by dashed lines in Fig. 1; otherwise it is of first order shown by thin solid lines. The tricritical point P which separates the first- and second-order phase transitions is located at $T = 0.079$ GeV and $\mu = 0.28$ GeV or $n_b/n_0 = 1.95$ with $n_0 = 0.17/\text{fm}^3$ being the baryon density in normal nuclear matter. Its positions in the T - μ and T - n_b planes are close to that calculated in the Landau ϕ^6 model and the instanton model [9].

At any critical point on the first-order phase-transition line in the T - μ plane, the thermodynamic potential as a function of the quark mass has two minima and one maximum between them. The coexistence of two minima indicates a mixed phase of chiral symmetry breaking and chiral symmetry restoration. The two spinodal points on the left hand and right hand sides of the maximum are characterized by a stability equal to zero,

$$\frac{\partial^2\Omega}{\partial m_q^2} = 0. \quad (5)$$

Between the spinodal points $\partial^2\Omega/\partial m_q^2 < 0$, the system is unstable with respect to a small fluctuation in quark mass. Outside the spinodal points and inside the minima $\partial^2\Omega/\partial m_q^2 > 0$, the system is metastable. In these regions a finite fluctuation in m_q may be amplified, and the system may not return to its original state after a sufficient deviation. Outside of the minima $\partial^2\Omega/\partial m_q^2 > 0$, the system is stable. The unstable and metastable regions are marked by US and MS in Fig. 1(b).

In the real world with nonzero current quark mass, the second-order phase transition becomes a smooth crossover and the tricritical point P becomes a critical end point E of a first-order phase-transition line. The end point E is a second-order critical point and shifted with respect to the tricritical point P towards larger μ in the T - μ plane and towards smaller n_b in the T - n_b plane. The first-order phase-transition lines are denoted by thick solid lines in the phase diagrams. Their shift with respect to the case of the chiral limit is due to the fact that it is more difficult for a phase transition to happen in a system of massive particles than that in the corresponding system of massless particles.

In the calculations of the phase-transition lines shown in Fig. 1, the three parameters in the NJL model, namely, the coupling constant G , the momentum cutoff Λ , and the current quark mass m_0 , are fixed by the constituent quark mass $m_q = 0.32$ GeV, the pion decay constant $f_\pi = 0.093$ GeV, and the pion mass $m_\pi = 0.134$ GeV (in the chiral limit $m_\pi = 0$) in the vacuum ($T = \mu = 0$). In the self-consistent mean field approximation, it is well known that the masses of the π and σ mesons satisfy the dispersion relation [4]

$$1 - 2G\Pi_M(T, \mu, m_M) = 0, \quad (6)$$

where m_M is the mass of the respective meson and Π_M is the associated retarded polarization function,

$$\begin{aligned} \Pi_\pi(T, \mu, m_\pi) &= N_c N_f \int \frac{d^3\mathbf{p}}{(2\pi)^3} \frac{1}{E_p} \frac{E_p^2}{E_p^2 - m_\pi^2/4} \\ &\quad \times \left[\tanh \frac{1}{2T}(E_p + \mu) + \tanh \frac{1}{2T}(E_p - \mu) \right], \\ \Pi_\sigma(T, \mu, m_\sigma) &= N_c N_f \int \frac{d^3\mathbf{p}}{(2\pi)^3} \frac{1}{E_p} \frac{E_p^2 - m_q^2}{E_p^2 - m_\sigma^2/4} \\ &\quad \times \left[\tanh \frac{1}{2T}(E_p + \mu) + \tanh \frac{1}{2T}(E_p - \mu) \right]. \end{aligned} \quad (7)$$

The pion coupling constant g_π is related to the residue at the pole of the pion propagator,

$$\begin{aligned} g_\pi^{-2} &= \frac{\partial \Pi_\pi(T, \mu, m_\pi)}{\partial m_\pi^2} \\ &= \frac{N_c N_f}{4} \int \frac{d^3\mathbf{p}}{(2\pi)^3} \frac{E_p}{(E_p^2 - m_\pi^2/4)^2} \left[\tanh \frac{1}{2T}(E_p + \mu) \right. \\ &\quad \left. + \tanh \frac{1}{2T}(E_p - \mu) \right]. \end{aligned} \quad (8)$$

It is easy to see that when $m_\pi > 2m_q$, $g_\pi = 0$, the pions will decay into quark-antiquark pairs, $\pi \rightarrow q\bar{q}$. Therefore, we can determine a hadronization line by

$$m_\pi(T_h, \mu_h) = 2m_q(T_h, \mu_h). \quad (9)$$

For temperature $T \geq T_h$ and chemical potential $\mu \geq \mu_h$ or baryon density $n_b \geq n_{bh}$, mesons become resonant states and no more pions exist in the model, and one has a system of interacting quarks. For $T \leq T_h$ and $\mu \leq \mu_h$ or $n_b \leq n_{bh}$, a quark-meson plasma is formed. This means that in the cooling process of relativistic heavy ion collisions the quark plasma begins to hadronize at the point (T_h, n_{bh}) . The coexistence of quarks and mesons at low temperature and density is of course an artifact of the NJL model.

In the chiral limit, Eq. (9) for determining the hadronization line is fully equivalent to the equation for defining the chiral phase-transition line. Therefore, the two lines coincide in the phase diagrams. When explicit chiral symmetry breaking is taken into account, the two equations become different. While there is no longer a phase transition at high temperature, one can still define the hadronization lines via Eqs. (9) and (4) which are shown in Fig. 1.

III. HADRONIZATION CROSS SECTION

The total hadronization cross section of a single quark in a flavor SU(2) model is defined as [7]

$$\sigma_q = \sigma_{u\bar{u} \rightarrow 2\pi_0} + \sigma_{u\bar{u} \rightarrow \pi_+ \pi_-} + \sigma_{u\bar{d} \rightarrow \pi_+ \pi_0}. \quad (10)$$

This is a measure of how quickly a quark hadronizes from a charge symmetric plasma. Since the NJL model is a strong-coupling theory, perturbation theory is inapplicable, and we require a selection procedure for the relevant Feynman graphs. We choose the $1/N_c$ expansion, and work to first order. To $O(1/n_c)$, the relevant T -matrix amplitudes for the reaction $q\bar{q} \rightarrow 2\pi$ are sketched in Fig. 2. It depicts the s -channel amplitude T^s in which an intermediate σ meson is produced and the t channel which displays a quark exchange. It is understood that the crossed diagrams are included for a process in which the final state particles are identical, e.g., for $u\bar{u} \rightarrow 2\pi_0$.

Using an obvious notation for the T -matrix amplitudes, one has for the process $u\bar{u} \rightarrow 2\pi_0$ the s -channel amplitude

$$T^s = \bar{v}(p_2)u(p_1) \frac{2G}{1-2G\Pi_\sigma(p_1+p_2)} g_\pi^2 \times A_{\sigma\pi\pi}(p_1+p_2, p_3) \delta_{c_1 c_2}, \quad (11)$$

where u and v are quark and antiquark spinors, the symbol $\delta_{c_1 c_2}$ refers to the color degree of freedom, and $A_{\sigma\pi\pi}$ represents the amplitude of the triangle vertex $\sigma \rightarrow \pi\pi$. By assuming the $q\bar{q}$ system to be at rest in the heat bath and evaluating the Matsubara sum in the triangle, one obtains the explicit dependence of the amplitude $A_{\sigma\pi\pi}$ on the Mandelstam Lorentz scalar $s = (p_1 + p_2)^2$ and the temperature T and chemical potential μ ,

$$A_{\sigma\pi\pi}(s, T, \mu) = 4m_q N_c N_f \times \int \frac{d^3\mathbf{p}}{(2\pi)^3} \frac{f_F(E_p - \mu) - f_F(-E_p - \mu)}{2E_p} \times \frac{8(\mathbf{p} \cdot \mathbf{p}_3)^2 - (2s + 4m_\pi^2)\mathbf{p} \cdot \mathbf{p}_3 + s^2/2 - 2sE_p^2}{(s - 4E_p^2)[(m_\pi^2 - 2\mathbf{p} \cdot \mathbf{p}_3)^2 - E_p^2 s]}, \quad (12)$$

where $\mathbf{p}_3^2 = \sqrt{s/4 - m_\pi^2}$, and the Fermi-Dirac distribution function $f_F(x) = (1 + e^{x/T})^{-1}$. In terms of the other two

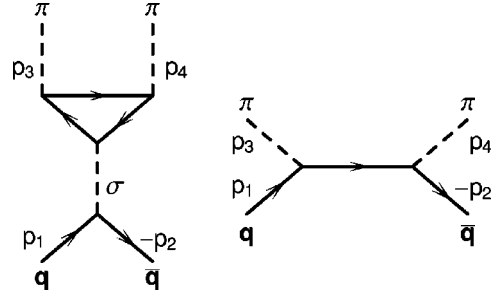


FIG. 2. The Feynman diagrams for the hadronization of a $q\bar{q}$ pair into two pions to the first order in $1/N_c$ expansion. The solid lines denote quarks and antiquarks; the dashed lines denote mesons.

Mandelstam variables $t = (p_1 - p_3)^2$ and $u = (p_1 - p_4)^2$ with the constraint $s + t + u = 2m_q^2 + 2m_\pi^2$, the direct and exchange contributions to the t -channel amplitude are

$$T^{t,dir} = \bar{v}(p_2) \gamma_5 \frac{\gamma^\mu (p_1 - p_3)_\mu + m_q}{t - m_q^2} \gamma_5 u(p_1) g_\pi^2 \delta_{c_1 c_2}, \quad (13)$$

$$T^{t,exc} = \bar{v}(p_2) \gamma_5 \frac{\gamma^\mu (p_1 - p_4)_\mu + m_q}{u - m_q^2} \gamma_5 u(p_1) g_\pi^2 \delta_{c_1 c_2}.$$

Since the s -channel crossed graph equals the direct term, the differential cross section can be written as

$$\frac{d\sigma_{u\bar{u} \rightarrow 2\pi_0}}{dt}(s, t, T, \mu) = \frac{1}{16\pi s(s - 4m_q^2)} \sum_{c,s}' |2T^s(s, T, \mu) + T^{t,dir}(t, T, \mu) + T^{t,exc}(u, T, \mu)|^2, \quad (14)$$

where the prime on the summation indicates the average over spin and color degrees of freedom of the quarks in the initial state.

It is necessary to note that in the s channel the triangle amplitude $A_{\sigma\pi\pi}$ and the σ polarization function Π_σ are both complex functions. Their real and imaginary parts are separated from each other by using the decomposition $1/(x + i\epsilon) = P(1/x) + i\pi\delta(x)$ for $A_{\sigma\pi\pi}(s + i\epsilon, T, \mu)$ and $\Pi_\sigma(s + i\epsilon, T, \mu)$.

After performing the integration over the momentum transfer t , the integrated cross section is obtained from

$$\sigma_{u\bar{u} \rightarrow 2\pi_0}(s, T, \mu) = \int_{t_{min}}^{t_{max}} dt \frac{d\sigma_{u\bar{u} \rightarrow 2\pi_0}}{dt}(s, t, T, \mu) \times \left[1 + f_B\left(\frac{\sqrt{s}}{2}\right) \right]^2, \quad (15)$$

where we have the limits $t_{max} = -\frac{1}{4}(s - 4m_q^2) - \frac{1}{4}(s - 4m_\pi^2) + \frac{1}{2}\sqrt{(s - 4m_q^2)(4 - m_\pi^2)}$, and $t_{min} = -\frac{1}{4}(s - 4m_q^2) - \frac{1}{4}(s - 4m_\pi^2)$ for the process $u\bar{u} \rightarrow 2\pi_0$ and $t_{min} = -\frac{1}{4}(s - 4m_q^2) - \frac{1}{4}(s - 4m_\pi^2) - \frac{1}{4}\sqrt{(s - 4m_q^2)(4 - m_\pi^2)}$ for the other

two processes. In Eq. (15) we have taken into account the Bose-Einstein distribution function $f_B(x) = (e^{x/T} - 1)^{-1}$ for the final state pions.

In the same way as Eq. (14) was constructed, we can write the differential cross sections for the processes $u\bar{u} \rightarrow \pi_+ \pi_-$ and $u\bar{d} \rightarrow \pi_+ \pi_0$ explicitly as

$$\frac{d\sigma_{u\bar{u} \rightarrow \pi_+ \pi_-}}{dt}(s, t, T, \mu) = \frac{1}{16\pi s(s - 4m_q^2)} \times \sum_{c,s}' |T^s(s, T, \mu) + 2T^{t,dir}(t, T, \mu)|^2,$$

$$\frac{d\sigma_{u\bar{d} \rightarrow \pi_+ \pi_0}}{dt}(s, t, T, \mu) = \frac{1}{16\pi s(s - 4m_q^2)} \times \sum_{c,s}' |\sqrt{2}T^{t,dir}(t, T, \mu)|^2. \quad (16)$$

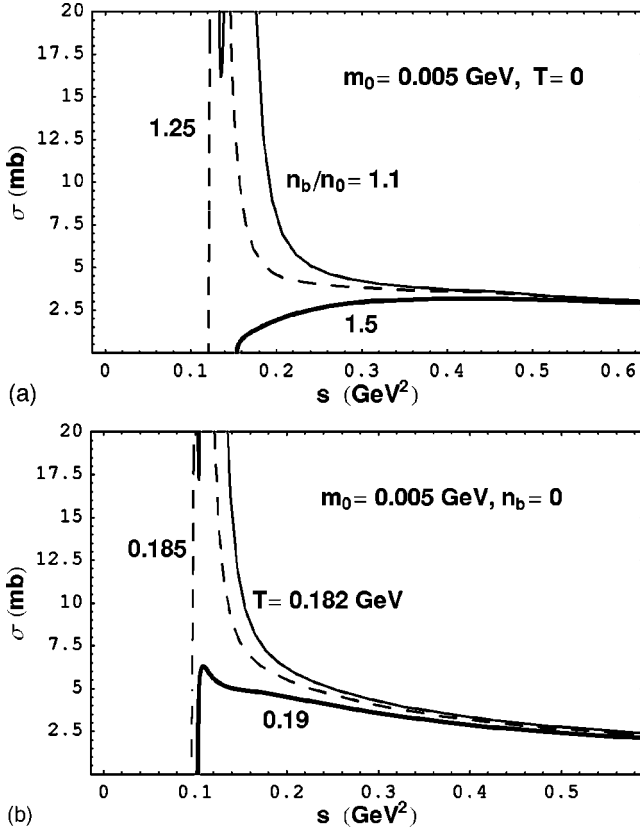


FIG. 3. The total hadronization cross section as a function of the collision energy s , for three different baryon densities (a) at $T=0$ and for three different temperatures (b) at $n_b=0$.

The total hadronization cross section discussed above in the whole $T-\mu$ (or $T-n_b$) plane and with explicit chiral symmetry breaking was studied in the chiral limit and along the T axis in Ref. [7]. The main result is the singularity structure of the cross section: $\sigma_q(s, T)$ displays singularities at the threshold energy $s_{th}=4m_q^2$ for any T and at the critical temperature T_c for any s . The singularity at s_{th} results from the fact that the entrance channel has a threshold energy s_{th} , while the exit channel has $s=0$. The singularity at T_c arises from the chiral symmetry restoration reflected on the quark exchange in the t channel: As $T \rightarrow T_c, m_q \rightarrow 0$, and then the amplitude $T^{t,dir} \rightarrow \infty$.

What we want to stress in this paper is the baryon density effect and the m_π dependence of the hadronization rate. Figure 3 shows the energy dependence of the integrated total cross section as a function of energy s for three values of the density n_b at zero temperature [Fig. 3(a)] and for three values of the temperature T at zero density [Fig. 3(b)]. Because of the three-momentum cutoff Λ , the energy range is restricted to $4[\text{Max}(m_q, m_\pi)]^2 \leq s \leq 4\{[\text{Max}(m_q, m_\pi)]^2 + \Lambda^2\}$. At low densities, there is still a kinematical divergence at $s_{th}=4m_q^2$ when $m_q > m_\pi$. For $n_b/n_0=1.1$, shown by the thin solid line in Fig. 3(a), the cross section drops down from infinity at $s_{th}=1.33 \text{ GeV}^2$ and then goes up again and reaches the second infinity at $s=m_\sigma^2$ which is the

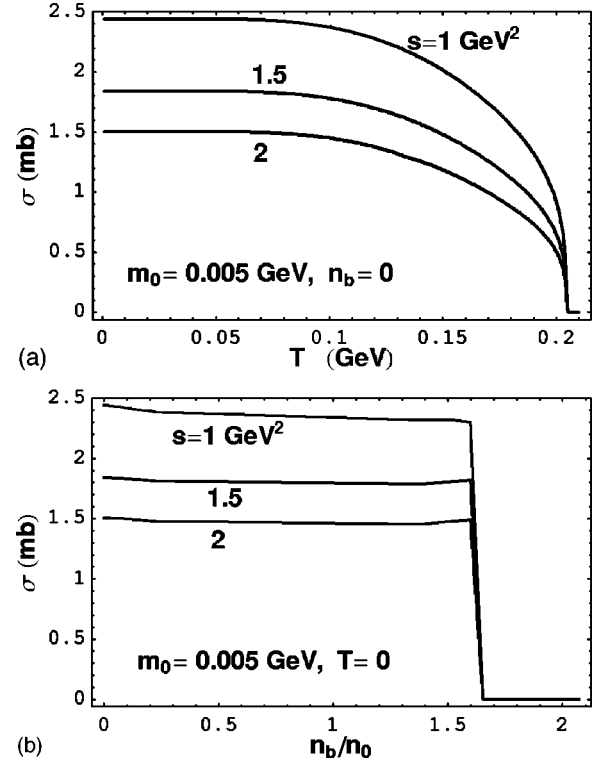


FIG. 4. The total hadronization cross section as a function of the temperature (a) at $n_b=0$ and as a function of the baryon density (b) at $T=0$. In each case, the collision energy takes three different values.

contribution from the σ exchange in the s channel. Then the cross section decreases and is fairly constant for large energies. With the increase of the density, when $m_\pi > m_q$, the threshold energy of the reaction is larger than the entrance energy, and therefore the first singularity disappears. In Fig. 3(a) this is the case for $n_b/n_0=1.25$ denoted by the dashed line. Further when the density is sufficiently high that the threshold energy $s=4m_\pi^2$ of the reaction is larger than m_σ^2 , the second singularity disappears too, and the cross section has no further singularities; see the thick solid line for $n_b/n_0=1.5$ in Fig. 3(a). The energy dependence of the cross section at finite temperature is similar and shown in Fig. 3(b).

The energy dependence of the singularity structure discussed here is very different from that in the chiral limit where there is always only one singularity at the threshold $s_{th}=4m_q^2$.

The temperature and density effects on the total cross section for three values of energy s are given in Fig. 4. At low density, the chiral phase transition is washed out in the case of a nonvanishing current quark mass $m_0=0.005 \text{ GeV}$, and so is the singularity in the cross section at the transition point. Even an expected maximum due to the small quark mass at this point does not exist. It reflects the chiral phenomenon that when the quark mass drops down with an increase of the temperature, the pion mass goes up simultaneously, and therefore it becomes more and more difficult for the quark plasma to hadronize into pions. At low tem-

perature, while the first-order phase transition remains, the dynamical singularity in the cross section is still washed out because of the finite quark and pion masses. However, very different from the temperature dependence shown in Fig. 4(a) where the quark plasma hadronizes smoothly and reaches the maximum rate within a temperature range $\Delta T \sim 0.1$ GeV, there is a hilly boundary in the $T-n_b$ plane [Fig. 4(b)] separating the quark-meson plasma at low density from the quark plasma at high density. This feature arises from the discontinuities of the quark and pion masses at the first-order phase-transition point. When the density decreases, the quark plasma first meets the hadronization point and begins to hadronize, and then it reaches the first-order phase transition; the sudden increase of the quark mass combined with the sudden decrease of the pion mass at the transition point leads to a jump in the cross section.

At zero temperature, the hadronization point and the chiral transition point are very close to each other (see Fig. 1; the quark plasma reaches the transition point immediately after the beginning of hadronization. Therefore, we see in Fig. 4(b) a precipitous jump from zero to a maximum for any s . The maximum, although it is not strong, is also a consequence of the discontinuities of the quark and pion masses at the transition point.

IV. CONCLUSIONS

The present investigation of the hadronization of a quark plasma in the NJL model to first order in $1/N_c$ has been motivated by two aspects: (1) The chiral symmetry restoration in the chiral limit and its consequence in the hadronization rate, a dynamical singularity at the critical point, are fully washed out when a nonvanishing current quark mass is taken into account. An important question is then what the influence of chiral dynamics is in the hadronization in the real quark world. (2) While the chiral phase transition happens at both high temperature and at high density, the order of the phase transition is different in the two cases. The second-order phase transition due to the temperature effect becomes a smooth crossover, but the first-order transition due to the density effect is retained when explicit chiral symmetry is considered. If such a first-order transition occurs in relativistic heavy ion collisions, we need to know what its experimental signatures are.

The NJL model may be used as a model of QCD as long as one is interested in the chiral properties of the quark world. In this model the hadronization point of the interacting quarks is above the chiral phase transition point in the

real world at high density, and the two points approach each other when the current quark mass goes to zero. Above the hadronization point one has a deconfined phase of quarks, but a quark-meson plasma below the point. Therefore, in the process of hadronization of the quark plasma, we expect that the retained first-order chiral transition at high density may still play an important role in the hadronization rate.

We have calculated the energy, temperature, and density dependence of the total hadronization cross section of a single quark in the framework of the flavor SU(2) NJL model. Corresponding to the motivations mentioned above, our main conclusions are the following: (1) The hadronization cross section is normally strongest for small values of the energy of the $q\bar{q}$ pair, and the singularity structure at low energies depends on the temperature and density. At low temperature or density, there are two singularities at the threshold energy and at the pole position (m_σ^2) of the σ propagator. As the temperature or density increases, the kinematical singularity at the threshold energy vanishes first when the pion mass m_π exceeds the quark mass m_q , and then the singularity at the pole disappears too when the threshold energy of the hadronization process, $s=4m_\pi^2$, is larger than m_σ^2 . As for the critical scattering, the divergence at the critical point for all values of s in the chiral limit is fully washed away. (2) Very different from the temperature effect which leads to a gradual hadronization during the cooling process of the quark plasma, the hadronization cross section is fairly constant in the process of hadronization at low temperature. The sudden jump of the cross section at the beginning of the hadronization means that the first-order transition of chiral symmetry restoration at high density is still reflected in the hadronization in the real quark world. A direct consequence of this feature is a suddenly strong increase of pion number in the expansion process of relativistic heavy ion collisions, if chiral symmetry is restored in the collisions. Our qualitative conclusions here derived from the NJL model may be more general because the first-order transition of chiral symmetry restoration looks like an essential feature of a strong interacting system at high density.

ACKNOWLEDGMENTS

We are grateful to S.P. Klevansky for a careful reading of the manuscript. The work was supported in part by the NSFC under Grant Nos. 19845001 and 19925519, and by the Major State Basic Research Development Program under Contract No. G2000077407.

-
- [1] B. Müller, Nucl. Phys. **A661**, 272 (1999); U. Hienz, hep-ph/9902424.
 [2] F. Karsch, in *Quark-Gluon Plasma*, edited by R.C. Hwa (World Scientific, Singapore, 1990), p. 61.
 [3] R. Rapp, T. Schäfer, E. Shuryak, and M. Velkovsky, Phys. Rev. Lett. **81**, 53 (1998); J. Berges and K. Rajagopal, Nucl. Phys. **B538**, 215 (1999).
 [4] For reviews and general references, see U. Vogl and W.

- Weise, Prog. Part. Nucl. Phys. **27**, 195 (1991); S.P. Klevansky, Rev. Mod. Phys. **64**, 649 (1992); M.K. Volkov, Prog. Part. Nucl. Phys. **24**, 35 (1993); T. Hatsuda and T. Kunihiro, Phys. Rep. **247**, 338 (1994).
 [5] R. Pisarski and F. Wilczek, Phys. Rev. D **29**, 338 (1984); K. Rajagopal, in *Quark-Gluon Plasma 2*, edited by R. C. Hwa (World Scientific, Singapore, 1995), p. 484.
 [6] H. Heiselberg and A.D. Jackson, nucl-th/9809013; T.M.

- Schwarz, S.P. Klevansky, and G. Papp, Phys. Rev. C **60**, 055205 (1999).
- [7] J. Hüfner, S.P. Klevansky, E. Quack, and P. Zhuang, Phys. Lett. B **337**, 30 (1994).
- [8] M. Asakawa and K. Yazaki, Nucl. Phys. **A504**, 668 (1989); P. Zhuang, J. Hüfner, and S.P. Klevansky, *ibid.* **A576**, 525 (1994); J. Hüfner, S.P. Klevansky, P. Zhuang, and H. Voss, Ann. Phys. (N.Y.) **234**, 225 (1994).
- [9] K. Rajagopal, hep-ph/9808348.